HAL
open science

# Non Linear Modulation of UHF Tag

Nicolas Barbot

## To cite this version:

Nicolas Barbot. Non Linear Modulation of UHF Tag. IEEE Journal of Radio Frequency Identification, 2023, 7, pp.38-44. 10.1109/JRFID.2022.3229204 . hal-04009038

**HAL Id: hal-04009038**

**https://hal.science/hal-04009038v1**

Submitted on 28 Feb 2023

**HAL** is a multi-disciplinary open access archive for the deposit and dissemination of scientific research documents, whether they are published or not. The documents may come from teaching and research institutions in France or abroad, or from public or private research centers.

L'archive ouverte pluridisciplinaire **HAL**, est destinée au dépôt et à la diffusion de documents scientifiques de niveau recherche, publiés ou non, émanant des établissements d'enseignement et de recherche français ou étrangers, des laboratoires publics ou privés.

# Non Linear Modulation of UHF Tag

Nicolas Barbot, *Member, IEEE*

***Abstract*—This paper presents a new modulation and detection scheme for UHF RFID tags. This detection method is not based on the load switching modulation classically used by the tag to communicate with the reader. The principle relies on the generation of a modulated signal by the reader combined with the non-linearity present in any RFID chip (or other non-linear devices). Under specific conditions, we show that the backscattered signal by the tag due to the non-linearity can produce new frequency components located around the carrier frequency used by the reader. These new components can be easily separated from the leakage and the response of the environment in the frequency domain. Moreover this detection can be done at a power which is significantly lower than the sensitivity of the chip. Thus, the associated detection range can be higher than the classical read range of the tag. In measurements, this detection range can be higher than 20 m for a fully passive tag and represents an enhancement of 30% compared to the classical read range.**

***Index Terms*—Linear time-variant system, non-linear systems, radar cross section, RFID, sensor.**

## I. Introduction

RADIO frequency identification is an essential technology to detect and identify numerous items at long distance and at high rate. The principle is based on the modulation of the scattered field by changing the load connected to an antenna as a function of time. This concept has been introduced by Stockman in 1948 [1]. An interesting point is that these devices can be fully passive if the power received from the reader can be harvested to realize the switching operation.

Note that all communications realized from the tag to the reader are based on the load switching modulation in which the tag can, when activated, switch the load connected to its antenna between two different impedance states. This load modulation allows one to transfer information from the tag to the reader but also to separate the contribution of the tag from the environment.

Read range of passive UHF tag is usually limited by the tag sensitivity $P_{tag}$ which corresponds to the minimum power needed to activate the tag. This sensitivity can be as high as $-10$ dBm for old chips (*e.g.*, Monza 1) and as low as $-22$ dBm for new chips (*e.g.*, Monza M700). The read range can be directly estimated based on the Friis equation [2]:

$$d_{rr} \leq \sqrt{\frac{P_t G_t G_{tag} \lambda^2}{(4\pi)^2 P_{tag}}} \tag{1}$$

The authors are with Univ. Grenoble Alpes, Grenoble INP, LCIS, F-26000 Valence, France.

where $P_t G_t$ is the maximum equivalent isotropically radiated power, $G_r$ is the gain of the tag antenna and $\lambda$ the wavelength. Note that for distances lower that (1), a UHF tag can be read (*i.e.*, its EPC value can be extracted by the reader) and detected (*i.e.*, presence or absence of the tag can be determined). Finally for distances higher that (1), tag can not be activated and consequently can not be read neither can be detected by any reader.

In this paper we demonstrate, for the first time, that it is possible to detect the presence of one (or several) UHF tag(s) at a distance higher than its (their) read range. This result is based on the non-linear behavior of any tag which appears even if the received power is lower than the tag sensitivity. The principle exploits both a specific modulated signal sent by the reader to the non-linear tag, and a detection method able to extract the non-linear tag response from the (linear) environment. We show that the chip non-linearity is able to generate new spectral components around the carrier frequency used by the reader. This response allows the reader to detect the presence of the tag at a distance which can be higher than the read range predicted by the Friis equation [see (1)].

Only few techniques in the literature have reported a detection method without using load modulation. In [3], [4], the authors generate a continuous wave at the fundamental frequency towards the tag and use the non-linearity of the chip to detect a power located at the harmonics of this fundamental frequency. However, conversion loss between the first and the third harmonic is generally prohibitive: $-57$ dB for classical tags [3], [5] and $-20$ dB for harmonic optimized tag [4] which significantly limits the performance of the approach. Also, dedicated antenna and RF path (with specific demodulation) are also needed to collect the power at the third harmonic and convert it to the baseband frequency to be used by the reader. Other techniques, based on intermodulation, have also been proposed to generate new frequency components around the carrier frequency [6], [7]. Intermodulation is also able to carry data like in [8]–[10] where a replica of the input signal at a slightly different frequency is backscattered by the transponder. Compared to [3]–[5], in the proposed method, all involved signals remain around the fundamental frequency which significantly reduces the complexity of the reading system. Compared to [6]–[10], all intermodulation terms are exploited to detect the presence of the non-linear tag.

The paper is organized as follows: Section II introduces the analytical model used to predict the behavior of the tag. Section III describes the detection method and the associated performance. Delta RCS and detection range associated to the non-linear modulation are also presented in Section III. Finally, Section IV concludes the paper.

Fig. 1. Equivalent circuit of a minimum scattering antenna with open circuit voltage $V_0(t)$ and loaded by a RFID chip $Z_c(t)$ exited by a modulated signal.

## II. Analytical Model

Let's consider a UHF tag modeled as a vertical half-wavelength dipole loaded with an impedance $Z_c$ in free space. This dipole is impinged by a plane wave vertically polarized, however, we do not restrict the study to a continuous wave excitation but we consider a narrow band electric field located around $f_0$. The associated analytic signal can be fully described by its complex envelope $E_0(t)$:

$$E^i(t) = E_0(t)e^{jkx}e^{2j\pi f_0 t}\,\hat{z} \tag{2}$$

where $k = 2\pi/\lambda$. The complex envelope of the open circuit voltage created at the load is directly linked to the effective length $l_e$ of the antenna [11]:

$$V_0(t) = E_0(t)\,l_e \tag{3}$$

Note that $|V_0(t)|$ is a function of the power received by the tag.

However, RFID chips are non-linear devices which means that the chip impedance $Z_c$ also depends on the received power. In the case of a modulated incident field, received power depends on time, thus $|V_0(t)|$ and $Z_c(t)$ are also both function of time. Note that $Z_c(t)$ can be seen as a specific load modulation due to the non-linear behavior of the tag and is the main topic of this article.

Since dipoles are minimum scattering antennas current can simply be extracted from an equivalent electric circuit [12]. Fig. 1 summarizes the different quantities for a modulated incident field $E^i(t)$. The current flowing into the dipole antenna $I(t)$ can then be expressed as:

$$I(t) = \frac{V_0(t)}{Z_a + Z_c(t)} = \frac{V_0(t)}{2R_a}\left(1 - \rho^*(t)\right) \tag{4}$$

The backscattered field $E^s(t)$ by the dipole can be written as:

$$E^s(t) = \frac{-j\eta k I(t) l_e(\theta) e^{-jkr}}{4\pi r} \tag{5}$$

Note that the variations of $Z_c(t)$, $\rho^*(t)$, $I(t)$, and $E^s(t)$ are not produced by the switching of the load at the tag side but by the combination of the modulated power sent by the reader and the non-linear behavior of the chip. In the general case, we can show that the spectrum of the scattered field $E^s(t)$ can have a different support compared to the spectrum of the incident field $E^i(t)$. This property allows one to detect the tag from the total received field (which can include leakage and reflections in the environment). Analytical expressions of the current $I(f)$ and scattered field $E^s(f)$ will be given in Section III. Finally, note that if a continuous wave is generated by the reader (which is the case for all UHF readers during tag replies), then $V_0$ and $Z_c$ are not function of time anymore and this non-linear modulation cannot be observed.

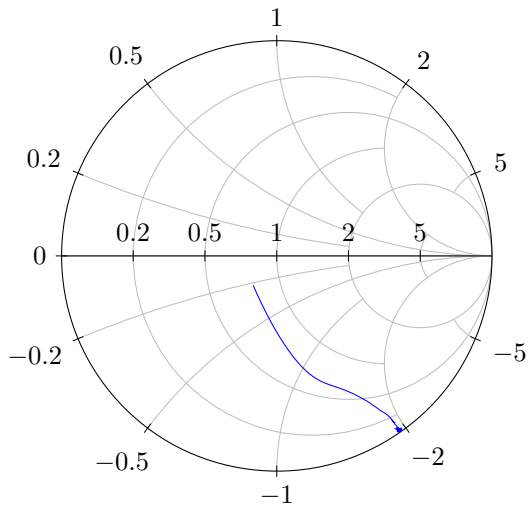


Fig. 2. Smith Chart of the $S_{11}$ parameter at 915 MHz with a power sweep from $-30$ dB to $-10$ dB for a NXP UCODE G2XM UHF RFID chips measured with the VNA.

This principle can also by viewed as a basic "communication" between the reader and the tag for which the reader send a given modulated signal towards the tag and the tag replies with a signal which is a function of the non-linear behavior of the chip. Note that this "communication" scheme is not based on the classical load modulation used by any UHF tag and is completely full-duplex (reader and tag operate at the same time). Also and more importantly, all the described operations can be realized at a power which is lower that the one needed to activate the chip. This last observation will allow one to extend the detection range at a distance higher than the tag read range. All these points will be developed in Section III.

## III. Results

### A. Chip Characterization

In order to characterize the chip impedance as a function of the incident power, we design a minimal printed circuit board with the chip connected to a SMA connector. $S_{11}$ parameter is measured using a Vector Network Analyzer (VNA). The chip under consideration is a NXP UCODE G2XM with a sensitivity of $P_{tag} = -15$ dBm. Note that other chips can be used and results (including model) presented here are valid for any chip. The power sweep was realized from $P = -30$ dBm to 10 dBm at 915 MHz and no matching network is added. Fig. 2 presents the $S_{11}$ parameter plotted in a Smith chart.

Note first that, since any (linear) impedance is independent of the input power value, it should appear as a point on the Smith chart. However, and as told in Section II, chip impedance is not linear as a function of the power, so the $S_{11}$ parameter is also a function of the power and describes a curve in the Smith chart. Note that both amplitude and phase of the reflected signal are modified during the power sweep.

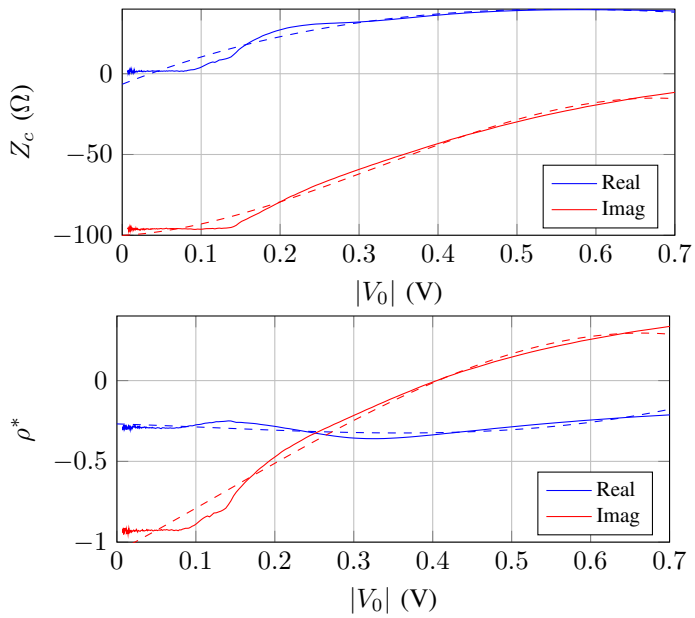


Fig. 3. (a) Impedance of the chip as a function of the magnitude of the open circuit voltage $|V_0|$. (b) Power wave reflection coefficient as a function of the open circuit voltage for a half-wave dipole antenna.

From Fig. 2, the chip impedance can be extracted and plotted as a function of the magnitude of the voltage $|V_0| = \sqrt{PR}$ where $R = 50\ \Omega$ is the impedance of the VNA. Results are presented for the chip impedance $Z_c$ [see Fig. 3(a)] and for the power wave reflection coefficient $\rho^*$ considering a dipole antenna of (linear) impedance $Z_a = 73 + j42.5\ \Omega$ [see Fig. 3(b)]. Finally, note that variation of $Z_c$ (or $\rho^*$) is continuous as a function of the power.

### B. Chip Modelization

We decide to model the values of $Z_c$ (or $\rho^*$) as a function of the magnitude of $V_0$ by a polynomial of degree $n$ of complex parameters $c_n$

$$Z_c(V_0) = \sum_{i=0}^{n} c_n |V_0|^n \tag{6}$$

$$\rho^*(V_0) = \sum_{i=0}^{n} c'_n |V_0|^n \tag{7}$$

Note that in this model, the impedance $Z_c(V_0)$ and reflection coefficient $\rho^*(V_0)$ do not depend on the phase of the complex envelope $V_0(t)$. This condition ensures that the chip impedance is only a function of the incident power and does not depend on the phase used by the reader. Coefficients $c_n$ (resp. $c'_n$) can be estimated by minimizing the mean square error between (6) [resp. (7)] and the measured values presented in Fig. 3(a) [resp. Fig. 3(b)]. Results are presented in Table I for the impedance $Z_c(V_0)$ and the power wave reflection coefficient $\rho^*(V_0)$ respectively for a maximum degree of $n = 3$. Coefficient $c_0$ represents the chip impedance value for low received power *i.e.*, when $|V_0|$ tends to zero. Polynomial values are also plotted in Fig. 3(a) and (b) in dashed. Note that the accuracy of the fitting can easily be increased with $n$ (especially around $|V_0| = 0$ V).

TABLE I
POLYNOMIAL CURVE FITTING FOR $Z_c(V_0)$ AND $\rho^*(V_0)$

| $n$ | 0 | 1 | 2 | 3 |
|---|---|---|---|---|
| $c_n$ | $-6.51-100j$ | $+192+28.7j$ | $-241-474j$ | $+82.7-489j$ |
| $c'_n$ | $-0.27-1.05j$ | $-0.16+2.60j$ | $-0.43-1.39j$ | $1.20-3.35j$ |

### C. Tag Signal Detection

Signal received by the reader corresponds the complex summation of the scattered field by the tag, a part of the incident field (leakage) and some possible reflections in the environment. The objective of this section is to determine an estimator allowing one to detect the presence of the tag among the total received signal. As we will see, this detection can be realized accurately in the frequency domain.

First, note that leakage and reflections have the same spectral components that the incident wave since they can all be described by linear time-invariant systems. However the spectrum of the backscattered signal by the tag can be different due to the non-linearity of the chip. This effect can actually be used to easily detect the presence of the non-linear tag inside the environment.

The spectrum of the signal backscattered by the tag $E^s(t)$ have the same components that the spectrum of $I(t)$. By taking the Fourier transform of (4), we have:

$$I(f) = \frac{V_0(f)}{2R_a} * [\delta(f) - \rho^*(f)] \tag{8}$$

$$= \frac{1}{2R_a} [V_0(f) - V_0(f) * \rho^*(f)] \tag{9}$$

Note that the first term of (9) has the same spectral components as $V_0(f)$ (and the transmitted signal) and can not be easily detected however, the second term is more interesting. The convolution $V_0(f) * \rho^*(f)$ can generate new spectral components in the current $I(f)$ and the backscattered field $E^s(f)$. These new components can easily be detected by the reader after the demodulation since they are not present in the transmitted signal.

Note that any modulation can be used on the reader side (as long as $|V_0(t)|$ is a function of time). However, amplitude modulations with sinusoidal variations producing a complex envelope of the form:

$$V_0(t) = a + b\cos 2\pi f_m t \tag{10}$$

where $a$ and $b$ are two constants, are good candidates since associated spectrum is equal to:

$$V_0(f) = a\delta(f) + \frac{b}{2}(\delta(f + f_m) + \delta(f - f_m)) \tag{11}$$

and has a support in the frequency domain restricted to $\pm f_m$ so new components can be easily detected after the convolution by $\rho^*(f)$.

Fig 4 presents the Fourier series of $V_0(t) = 0.35 + 0.35\cos 2\pi f_m t$ which is the complex envelope of a double-sideband with carrier modulation (*i.e.*, full AM modulation), $\rho^*(t)$, and the current $I(t)$, for both measured values and polynomial approximation. Note that, measurement and model are in a good agreement, thus the proposed model can be used

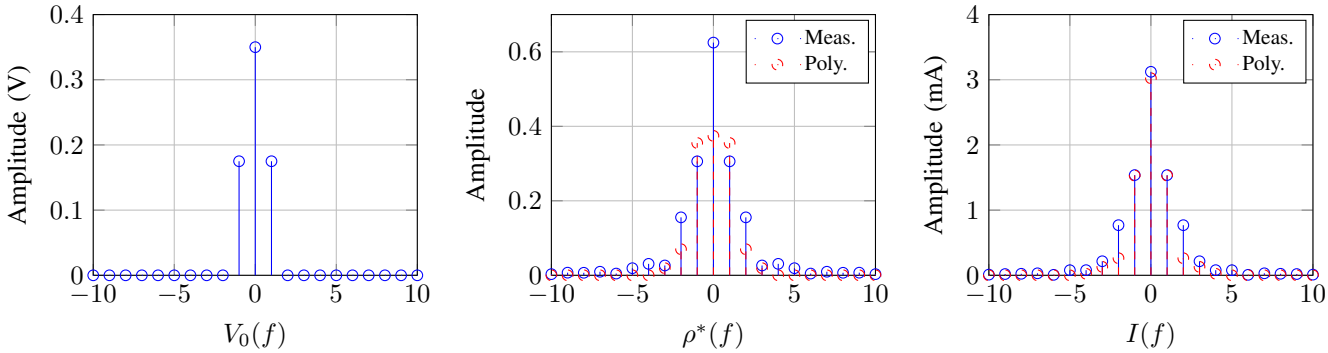


Fig. 4. Fourier series of (a) $V_0(t) = 0.35 + 0.35(\cos 2\pi f_m t$ (which is the complex envelope of a double-sideband with carrier), (b) $\rho^*(t)$, and (c) $I(t)$, for both measured values and polynomial approximation.

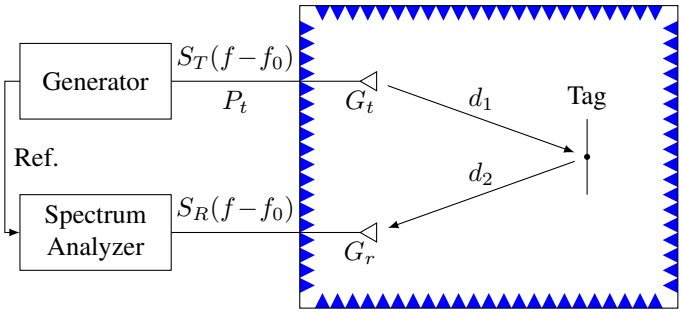


Fig. 5. Measurement bench used to measure the scattered field of UHF tag.

TABLE II
UHF TAGS UNDER CONSIDERATION IN THIS STUDY.

| | Manufacturer | Model | Chip |
|---|---|---|---|
| Tag 1 | Avery Dennison | AD-61-5 | MB97R803A |
| Tag 2 | Custom | FR4 (0.8 mm) | XRAG2 |
| Tag 3 | Rafsec | Dogbone | Monza 1 |
| Tag 4 | Intermec | AD-222 | Monza 2 |
| Tag 5 | Alien | 2015 | Higgs-EC |
| Tag 6 | LAB ID | 106HU | Monza R6 |

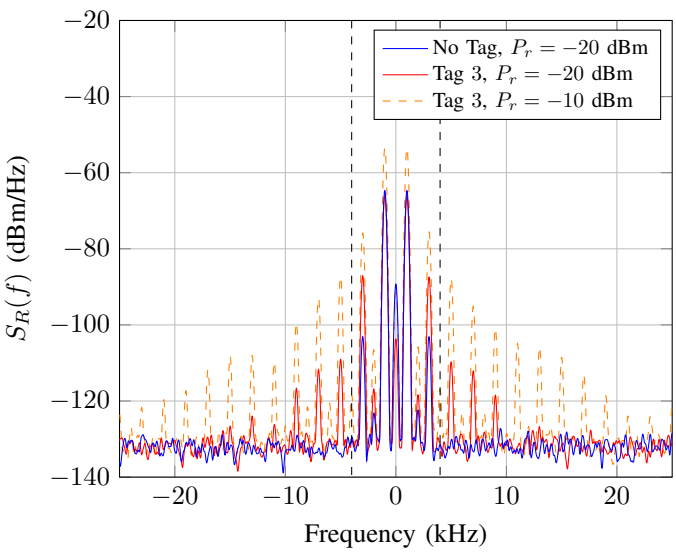


Fig. 6. Spectrum without tag at $P_t = 0$ dBm (corresponding to $P_r = -20$ dBm) and with Tag 3 and $P_t = 0$ and 10 dBm (corresponding to $P_r = -10$ dBm), at $f_0 = 915$ MHz in anechoic chamber. Modulated incident field is based on double-sideband suppressed carrier modulation.

to predict the frequency components of $I(t)$. Finally, since the scattered field $E^s(t)$ is proportional to $I(t)$, we can see that the tag can backscatter power at frequencies which are different that the ones used by the reader (*i.e.*, at $\pm n f_m$ with $n \geq 2$). These components are only generated by the tag and can easily be separated from the leakage and reflections from the environment.

### D. Measurement Bench

Measurement bench is presented in Fig. 5 and corresponds to a bistatic configuration. Emission is based on a vector generator (Agilent N5182A) and a power amplifier (EMPOWER 2053-BBS3I4AAJ) to transmit the modulated incident field around the carrier frequency $f_0 = 915$ MHz at a power of $P_t$ in the interval $[-10; +30]$ dBm. Reception is realized by a spectrum analyzer (Tektronix RSA 3408A) at $f_0 = 915$ MHz over a span of $2b = 50$ kHz. Both instruments use the same 10 MHz reference signal. Note that a monostatic configuration can also be used with a circulator or a directional coupler. The tag is placed at a distance of $d_1 = d_2 = 1.5$ m in an anechoic environment, in the farfield zone of the antennas (AH Systems inc. SAS-571). Note that simple narrow band antennas can be used since all involved signals are located around $f_0$. Finally and unless otherwise specified, the generator transmits a double-sideband suppressed carrier modulation [*i.e.*, with $a = 0$ and $b = 1$ in (10)] with $f_m = 1$ kHz.

For the tags used in this study, we have considered 6 different UHF tags. Note that any tag can be used since all tags are non-linear devices. Table II presents the different tags.

Backscattered field can be measured using the test-bench presented in Fig. 5. Results without and with a single UHF tag (Tag 3) are displayed in Fig. 6 at $f_0 = 915$ MHz, for a received power of $-20$ dBm at the tag side. Note that the received signal when no tag is present is simply a scaled version of the modulated transmitted signal. This signal presents a slight distortion since harmonics are present

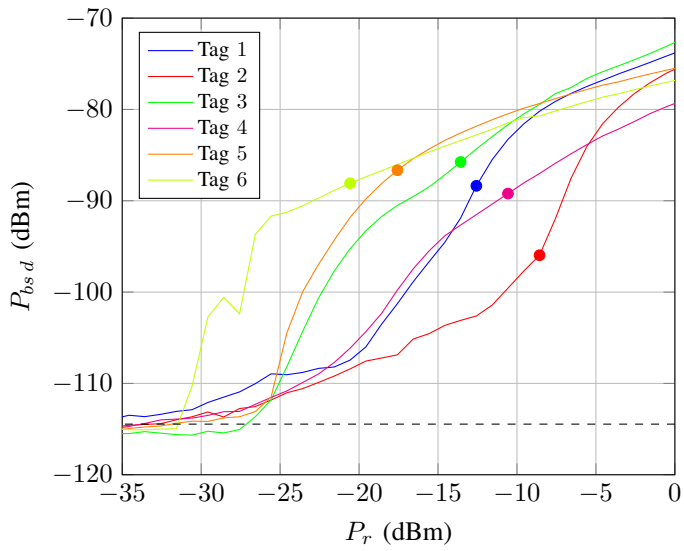


Fig. 7. Modulated power backscattered by the different tags as a function of the received power at 915 MHz in anechoic chamber. Modulated incident field is based on double-sideband suppressed carrier modulation. Circle markers represent the sensitivity (activation power) for each tag.

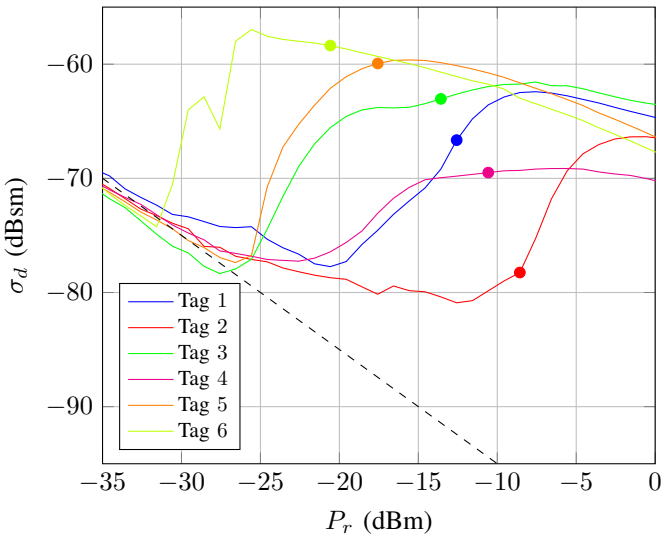


Fig. 8. Delta RCS of the different tags as a function of the received power by the tag at 915 MHz in anechoic chamber. Modulated incident field is based on double-sideband suppressed carrier modulation. Circle markers represent the sensitivity (activation power) for each tag.

TABLE III
TAG SENSITIVITY AND MINIMUM RECEIVED POWER NEEDED TO DETECT THE MODULATION DUE TO THE NON-LINEARITY.

| | $P_{tag}$ (dBm) | $P_{tag\,nl}$ (dBm) |
|---|---|---|
| Tag 1 | −13 | −32 |
| Tag 2 | −8.3 | −14 |
| Tag 3 | −14 | −26 |
| Tag 4 | −11 | −24 |
| Tag 5 | −18 | −25 |
| Tag 6 | −21 | −31 |

at $\pm 3f_m$ due to non-linearity and imperfection of the generator and amplifier. Moreover, an offset is visible at 0 Hz due to the leakage and the residual reflections present in the anechoic chamber. However, when Tag 1 is present in the environment, received spectrum presents new components located at $\pm nf_m$ with $n \geq 2$. Similar results are also observed when multiple tags are present in the environment. The observed spectrum is in agreement with the spectrum of the current presented in Fig 4(c). Moreover this behavior is all the more visible when the transmitted power is increased (both in term of amplitude and number of peaks). Finally, note that the tag can be detected at a power which is lower that its sensitivity (*e.g.*, Rafsec Dogbone with Monza 1 chip has a sensitivity of $P_{tag} = -14$ dBm). This result has significant consequences of the range at which a tag can be detected by the proposed method.

### *E. Delta RCS*

The modulated power which can be detected by the reader can be linked to the differential RCS $\sigma_d$ associated to the non-linear behavior of the UHF tag. Differential RCS has been introduced in [13] to characterize the modulated power backscattered by the tag during the classical switching operation. However, this definition has been generalized to any modulated tag in [14] based on a frequency domain definition. This new definition can directly be applied to the modulation generated by the non-linear behavior of the tag by removing the power in the band $[-\epsilon; +\epsilon]$ around the carrier frequency $f_0$ used by the reader.

Measurement bench is identical as the one described in Fig. 5. Differential RCS can be estimated by [14]:

$$\sigma_d = \frac{(4\pi)^3 d_1^2 d_2^2}{P_t G_t G_r \lambda^2} \times \left[ \int_{f_0-b}^{f_0-\epsilon} S_R(f - f_0)\,\mathrm{d}f + \int_{f_0+\epsilon}^{f_0+b} S_R(f - f_0)\,\mathrm{d}f \right] \quad (12)$$

where the second term corresponds to the modulated power $P_{bs\,d}$ received at the reader side. Modulation done by the reader is removed over a bandwidth of $2\epsilon = 7$ kHz (see dashed lines in Fig. 6). This value is higher than the minimal bandwidth of 3 kHz but allows one to remove the distortion observed in Fig. 6 at a price of a lower modulated power and delta RCS value. Note that this bandwidth allows the reader to separate the contribution of the leakage and the reflections from the environment to keep only the spectral components associated to the modulated power backscattered by the tag.

Fig. 7 presents the modulated power $P_{bs\,d}$ scattered by the tag towards the reader as a function of the maximum received power by the tag (which is obtained using the Friis equation). We can see that the modulated power is an increasing function of the received power. Moreover, this modulated power can be detected even if the received power by the tag is lower than its sensitivity (see circle markers for each tag in Fig. 7). For example, Tag 6 can be detected with a received power of $P_{tag\,nl} = -31$ dBm whereas its sensitivity is $P_{tag} = -21$ dBm.

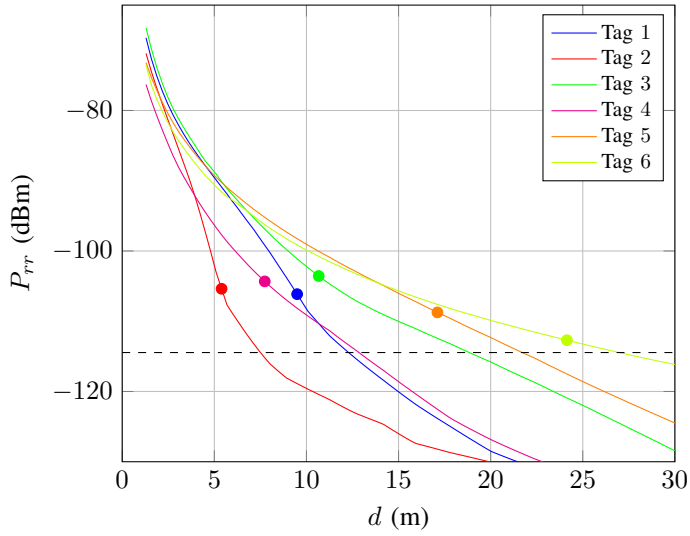


Fig. 9. Modulated power received at the reader side as a function of the equivalent distance for a EIRP of 36 dBm at 915 MHz considering $G_t = G_r = 7$ dBi. Detection range can be determined with the intersection with the minimum detectable modulated power $P_{rr\,min}$ (dashed line).

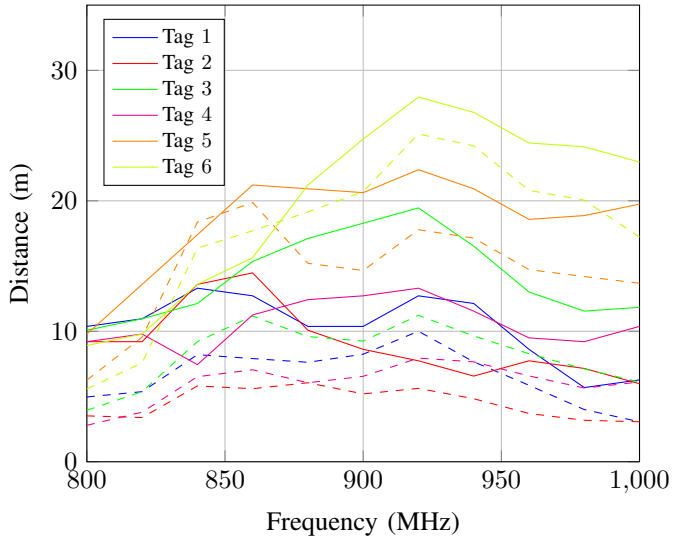


Fig. 10. Comparison between the detection range (plain line) and the read range (dashed line) for the considered tags as a function of the frequency.

Table III presents a comparison between the sensitivity of the tag $P_{tag}$ (*i.e.*, the minimum received power needed to activate a tag and be able to reply to a Gen2 command), and the minimum power needed to detect the presence of the tag when a double band suppressed carrier modulation is used at the reader side $P_{tag\,nl}$. We can see that this power is in average 10 dB lower than the sensitivity of the tag. As we will see, this result will have significant consequences over the range at which a tag can be detected based on its non-linear behavior.

Differential RCS can now be computed for the non-linear modulation. Note first that for UHF tags in classical operation (*i.e.*, load switching modulation), $\sigma_d$ is a quantity almost constant as a function of the received power when the tag is modulating and is equal to zero when the tag is not activated. (In practice, $\sigma_d$ is a slightly decreasing function of the received power since tags include a shunt resistance to avoid overvoltage when placed in close proximity of the reader antenna [15].) Differential RCS associated to the non-linear behavior of the tag is plotted as a function of the maximum received power by the tag in Fig. 8. Note that this delta RCS strongly depends on the power received by the tag. The results also depend on the chip architecture and vary with the considered tag. The dashed line represents the minimum $\sigma_d$ which can be measured for a noise of power spectral density of $N_0 = -131$ dBm/Hz (see Fig. 6). All values above this line can be detected by the spectrum analyzer.

### *F. Detection Range*

The range at which the non-linear behavior of the tag can be detected is different than the classical read range at which the tag can be read in an inventory round (as defined in the EPC Gen 2 protocol).

For passive tags based on load switching modulation, read range is usually limited by the power received by the tag and can be estimated, in free space, using Friis equation [see (1)]. However, when the proposed modulation scheme is used by the reader, non-linear modulation of the tag can appear at a power which can be more than 10 dB lower than the activation power. In this case, the detection range is not limited by the tag sensitivity anymore but by the reader sensitivity and can be estimated, in free space, by the radar equation [16]:

$$d_{dr} \leq \sqrt[4]{\frac{P_t G_t G_r \lambda^2 \sigma_d}{(4\pi)^3 P_{rr\,min}}} \tag{13}$$

where $P_{rr\,min}$ is the minimum modulated power which can be detected by the reader.

Detection range is also harder to estimate since, as shown in Fig. 8, $\sigma_d$ is a function of the power received by the tag. Note however that the detection sensitivity $P_{rr\,min} = 2N_0(b - \epsilon)$ is usually lower than classical reader sensitivity since the required bandwidth is smaller (50 kHz and 4 BLF respectively [14]).

Results, in anechoic chamber, are presented in Fig. 9 for the different tags at 915 MHz considering $G_t = G_r = 7$ dBi. For the read range, a query command is generated using the vector generator, read range is extracted from the minimum power at which the RN16 can be detected by the spectrum analyzer. For the detection range, a double-sideband suppressed carrier modulation [*i.e.*, with $a = 0$ and $b = 1$ in (10)] is generated and the tag is detected based on the presence of the harmonics at $f_0 \pm 3f_m$. Note that the exact same instruments and configuration are used for both ranges. We can see that detection range is higher than the read range for all considered tags. In average, detection range corresponds to an improvement of 30% compared to the read range.

Detection range and read range are compared in Fig. 10 between 800 and 1000 MHz in anechoic chamber. Antenna gains at the reader side have been taken into account over the entire bandwidth. We can see that detection range is higher than the read range for all tags in all the considered bandwidth. This improvement corresponds to a increase of 5 m compared

TABLE IV
READ RANGE $d_{rr}$ IN FREE SPACE (FS) AND REAL ENVIRONMENT (OE) AND DETECTION RANGE $d_{dr}$ IN REAL ENVIRONMENT AT 915 MHZ AND AN EIRP OF 22 DBM.

| | $d_{rr\,fs}$ (m) | $d_{rr\,oe}$ (m) | $d_{dr\,oe}$ (m) |
|---|---|---|---|
| Tag 1 | 1.9 | 1.1 | 2.4 |
| Tag 2 | 1.1 | 0.9 | 1.1 |
| Tag 3 | 2.1 | 1.1 | 2.5 |
| Tag 4 | 1.5 | 1.2 | 1.9 |
| Tag 5 | 3.3 | 1.5 | 2.3 |
| Tag 6 | 4.7 | 2.6 | 6.0 |

to the read range. These results validate the performance of the proposed approach.

Finally, measurements have also been reported in real environment using the same measurement bench than the one used in anechoic chamber. Read range and detection range have been determined with an EIRP of 22 dBm, by moving the considered tag away form the reader. Note that this low power value was chosen to limit the distortion of the power amplifier. Results in real environment, for read range and detection range, are presented in Table IV and compared to the read range obtained in free space using Friis equation [see (1)]. Real environment affects both ranges due the multipath propagation however, we can see that the detection range is still higher that the read range in real environment. Moreover, for a given tag, a similar improvement factor can be observed in free space (Fig. 9) and in real environment. This remark holds for all the tags.

Note that the proposed method can allow one to detect tag at a distance which can be higher than the one required to activate the tag. Thus, assuming a perfectly linear power amplifier, it can be possible to detect a tag based on the proposed method before being able to identify it using classical Gen2 commands.

## IV. CONCLUSION

This paper presents a method able to detect the presence of a tag at a distance higher than its read range. The principle is based on the non-linear behavior of the tag and can be realized by simply modulating the transmitted power of the reader. Results show that it is possible to detect a tag at a distance higher than 20 m. Thus, the paper shows that it is possible to detect the presence of a tag (with a slowly modulated field) before being able to read it (with the classical Gen 2 commands).

## REFERENCES


[1] H. Stockman, "Communication by means of reflected power," *Proceedings of the IRE*, vol. 36, no. 10, pp. 1196–1204, Oct. 1948.

[2] H. Friis, "A note on a simple transmission formula," *Proceedings of the IRE*, vol. 34, no. 5, pp. 254–256, May 1946.

[3] P. V. Nikitin and K. V. S. Rao, "Harmonic scattering from passive UHF RFID tags," in *2009 IEEE Antennas and Propagation Society International Symposium*, North Charleston, SC, Jun. 2009, pp. 1–4.

[4] G. Andíia Vera, Y. Duroc, and S. Tedjini, "Third harmonic exploitation in passive UHF RFID," *IEEE Trans. Microw. Theory Techn.*, vol. 63, no. 9, pp. 2991–3004, 2015.

[5] G. Andía Vera, Y. Duroc, and S. Tedjini, "Analysis of harmonics in UHF RFID signals," *IEEE Trans. Microw. Theory Techn.*, vol. 61, no. 6, pp. 2481–2490, 2013.

[6] V. Viikari and H. Seppa, "RFID MEMS sensor concept based on intermodulation distortion," *IEEE Sensors Journal*, vol. 9, no. 12, pp. 1918–1923, Oct. 2009.

[7] P. Pursula, N. Pesonen, I. Marttila, J. Song, and V. Viikari, "Achieving long reading ranges with passive wireless intermodulation sensors," in *2014 IEEE RFID Technology and Applications Conference (RFID-TA)*, Tampere, Finland, Sep. 2014, pp. 131–134.

[8] H. C. Gomes and N. B. Carvalho, "The use of intermodulation distortion for the design of passive RFID," in *2007 European Radar Conference*, Munich, Germany, Oct. 2007, pp. 377–380.

[9] H. Gomes and N. Carvalho, "RFID for location proposes based on the intermodulation distortion," *Sensors & Transducers Magazine*, vol. 106, no. 7, pp. 85–96, July 2009.

[10] Y. Qaragoez, S. Pollin, and D. Schreurs, "Enhanced two-way communication for battery-free wireless sensors: SWIPT with IM3 backscattering," in *2022 IEEE MTT-S International Microwave Symposium (IMS)*, Denver, CO, Jul. 2022, pp. 1–1.

[11] C. A. Balanis, *Antenna theory: analysis and design*. John wiley & sons, 2015.

[12] R. Harrington, "Electromagnetic scattering by antennas," *IEEE Trans. Antennas Propag.*, vol. 11, no. 5, pp. 595–596, Sep. 1963.

[13] P. Nikitin, K. V. S. Rao, and R. D. Martinez, "Differential RCS of RFID tag," *Electron. Lett.*, vol. 43, no. 8, pp. 431–432, Apr. 2007.

[14] N. Barbot, O. Rance, and E. Perret, "Differential RCS of modulated tag," *IEEE Trans. Antennas Propag.*, vol. 69, no. 9, pp. 6128–6133, Sep. 2021.

[15] E. Colin, A. Moretto, C. Ripoll, and S. A. Chakra, "Delta RCS of UHF RFID taking into account the shunt resistance in the tag model," in *2009 Joint IEEE North-East Workshop on Circuits and Systems and TAISA Conference*, Toulouse, France, Jun. 2009, pp. 1–4.

[16] N. Barbot, O. Rance, and E. Perret, "Classical RFID vs. chipless RFID read range: Is linearity a friend or a foe?" *IEEE Trans. Microw. Theory Techn.*, vol. 69, no. 9, pp. 4199–4208, Sep. 2021.


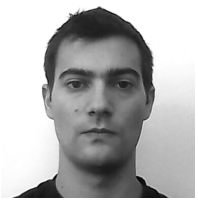


**Nicolas Barbot** (Member, IEEE) received the M.Sc. degree and Ph.D. degree from the University de Limoges, France in 2010 and 2013 respectively. His Ph.D. work in Xlim Laboratory was focused on error-correcting codes for the optical wireless channel. He also realized a post-doctoral work in joint source-channel decoding at L2S Laboratory, in Gif-sur-Yvette, France. Since September 2014, he has been an Assistant Professor at the Université Grenoble Alpes - Grenoble Institute of Technology, in Valence, France. His scientific background at LCIS Laboratory covers wireless communications systems based on backscattering principle which include classical RFID and chipless RFID.

His research interests include transponders which can not be described by linear time-invariant systems. This gathers harmonic transponders which are based on the use of a non-linear component (Schottky diode) or linear time-variant transponders which are based on the modification of their response in the time domain. He also places special interests on antenna design and instrumentation based on these phenomena.